Supplementary Materials for: Role of sources and atmospheric sink on seasonal cycle of CH_4 and δ^{13}-CH_4: analysis based on atmospheric chemistry transport model

Vilma Kangasaho[1], Aki Tsuruta[1], Leif Backman[1], Pyry Mäkinen[2], Sander Houweling[3,4], Arjo Segers[5], Maarten Krol[6,7], Ed Dlugokencky[8], Sylvia Michel[9], James White[9], and Tuula Aalto[1]

[1]Finnish Meteorological Institute, P.O. Box.503, FI-00101, Helsinki, Finland
[2]Aalto University, Finland
[3]SRON Netherlands Institute for Space Research, the Netherlands
[4]Vrije Universiteit Amsterdam, the Netherlands
[5]Netherlands Organisation for Applied Scientific Research (TNO), Utrecht, the Netherlandss
[6]Wageningen University & Research, Meteorology and Air Quality, the Netherlands
[7]IMAU, Utrecht University, the Netherlands
[8]NOAA Global Monitoring Laboratory (GML), USA
[9]NSTAAR, University of Colorado, USA

Correspondence: Vilma Kangasaho (vilma.kangasaho@fmi.fi)

Table S1. IPCC CH_4 source division based on 1996 Guidelines (Houghton et al., 1997)

	IPCC class
Energy	**1**
Fuel Combustion Activities	1A
Energy Industries	1A1
Manufacturing Industries and Construction (ISIC)	1A2
Transport	1A3
Civil Aviation	1A3a
Road Transportation	1A3b
Railways	1A3c
Navigation	1A3d
Other Transportation	1A3e
Other Sectors	1A4
Fugitive Emissions from Fuels	1B
Solid Fuels	1B1
Oil and Natural Gas	1B2
Oil	1B2a
Natural Gas	1B2a
Solvent and Other Product Use	**2**
Chemical Industry	2B
Metal Industry	2C
Agriculture	**4**
Enteric Fermentation	4A
Manure Management	4B
Rice Cultivation	4C
Agricultural Soils	4D
Waste	**6**
Solid Waste and Disposal on Land	6A
Waste Water Handling	6B
Waste Incineration	6C
Other	6D
Other	**7**
Fossil Fuel Fires	7A

Table S2. Sectors formed in this study based on EDGAR database and IPCC classification.

Sector	**EDGAR 4.3.2**	**EDGAR 5.0**
Enteric Fermentation and Manure Management	4A, 4B	4A, 4B
Landfills and Waste Water Treatment	6A, 6B, 6C, 6D	6A, 6B, 6C, 6D
Rice cultivation	4C, 4D1, 4D2, 4D4	4C, 4D
Coal	1B1a	1B1a
Oil and Gas	1B2a1, 1B2a2, 1B2a3, 1B2a4, 1B2c, 1A3a_CDS, 1A3a_CRS, 1A3aLTO, 1A3a_SPS, 1A3c, 1A3e, 1A3d, 1A3b, 2B, 2C1c, 2C1d, 2C1e, 2C1f, 2C2, 1A1a, 1A2, 1A1b, 1A1c, 1A5b1, 1B1b, 1B2a5, 1B2a6, 1B2b5, 2C1b,7A	1A1a, 1A1b, 1A1c, 1A5b1, 1B1b, 1B2a5, 1B2a6, 1B2b5, 2C1b, 1A2, 1A3a_CDS, 1A3a_CRS, 1A3a_LTO, 1A3b, 1A3c, 1A3e, 1A3d, 1C2, 1B2a1, 1B2a2, 1B2a3, 1B2a4, 1B2c, 2B, 2C1a, 2C1c, 2C1d, 2C1e, 2C1f, 2C2, 7A
Residential	1A4	1A4

Table S3. Average global emission amplitude (Tg CH_4 $month^{-1}$), and the months when seasonal minimum and maximum occurs. For EDGAR components, those for 2010 and 2015 for v4.3.2 and v5.0 are shown, respectively. For natural sources, the variation shows those between different years. Those marked with "*" does not have monthly variations. Note that geological and termite emissions do not have seasonal variability, and thus not included in this table.

Data source	Component	Amplitude	MIN	MAX
EDGAR v4.3.2	Enteric Fermentation and Manure Management (EFMM)	7.50	Nov.	Mar.
	Landfills and Waste Water Treatment (LWW)	*	*	*
	Rice (RICE)	2.61	Jan., Dec.	Mar.
	Coal	0.03	Jul.	Jan.
	Oil and Gas	0.07	Jul.	Nov.
	Residential	0.78	Jul.	Jan.
EDGAR v5.0	Enteric Fermentation and Manure Management (EFMM)	*	*	*
	Landfills and Waste Water Treatment (LWW)	*	*	*
	Rice	5.51	Mar.	Aug.
	Coal	*	*	*
	Oil and Gas	0.10	Sep.	Jan.
	Residential	1.65	Sep.	Jan.
LPX-Bern v1.4	Wetland	8.55	Nov., Dec.	Jul., Aug.
LPX-Bern v1.4	Soil sink	0.99	Jul.	Jan., Feb.
GFED v4.2	Fires	2.44	Feb.–Apr., Nov.	Jun.–Aug.
Tsuruta et al. (2017)	Ocean	0.08	Feb., Apr.–Jun., Nov.	Jan., Mar., Jul., Aug., Oct., Nov.

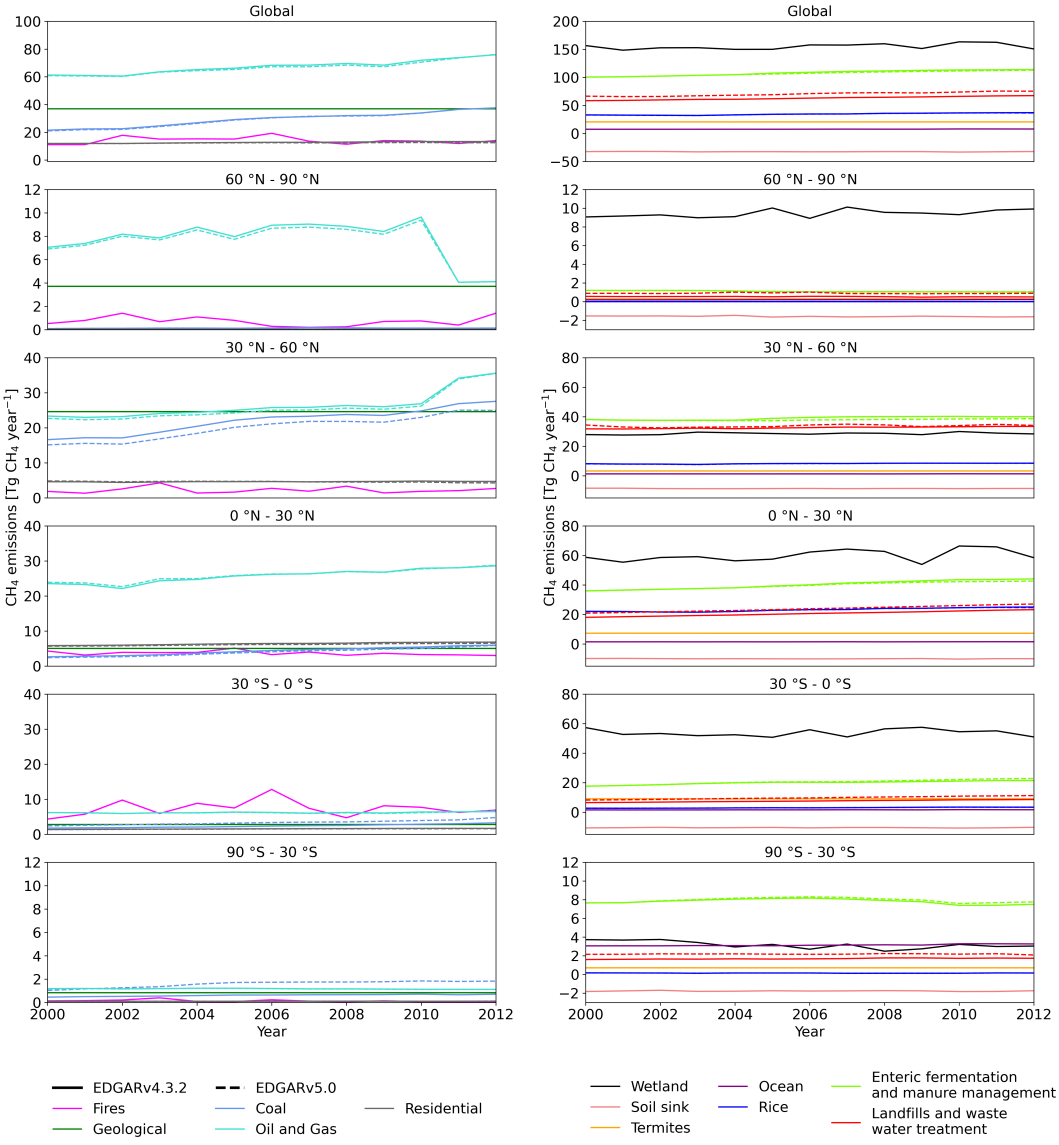

Figure S1. Annual total global (top) and latitudinal zonal total CH_4 emissions during 2000–2012. The left-hand side panel includes fossil-based emissions and the right-hand side panel emissions from biogenic origin, both natural and anthropogenic. Global emissions (top) are split into 30° latitude bands.

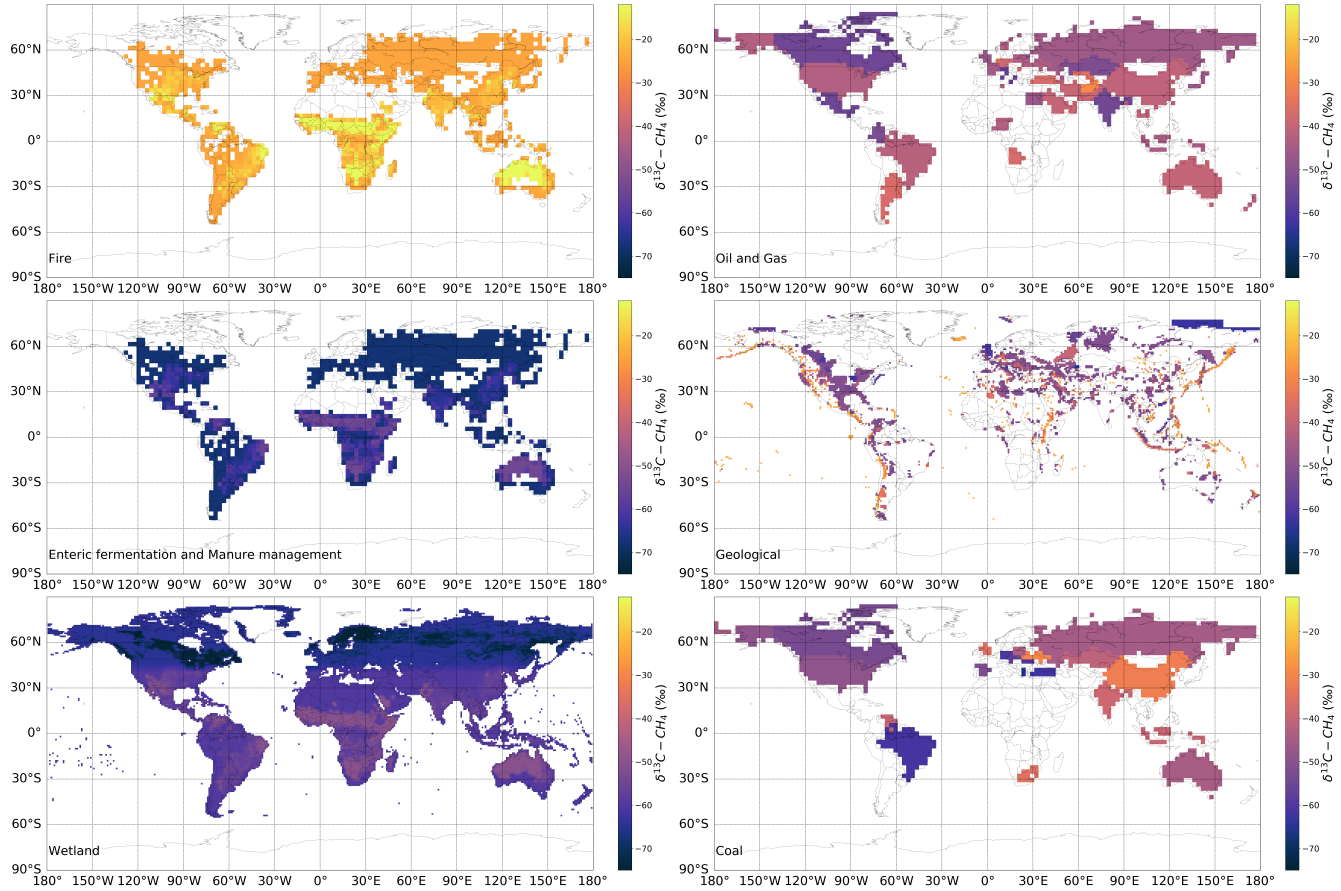

Figure S2. Spatially varying isotopic signature values used in simulations.

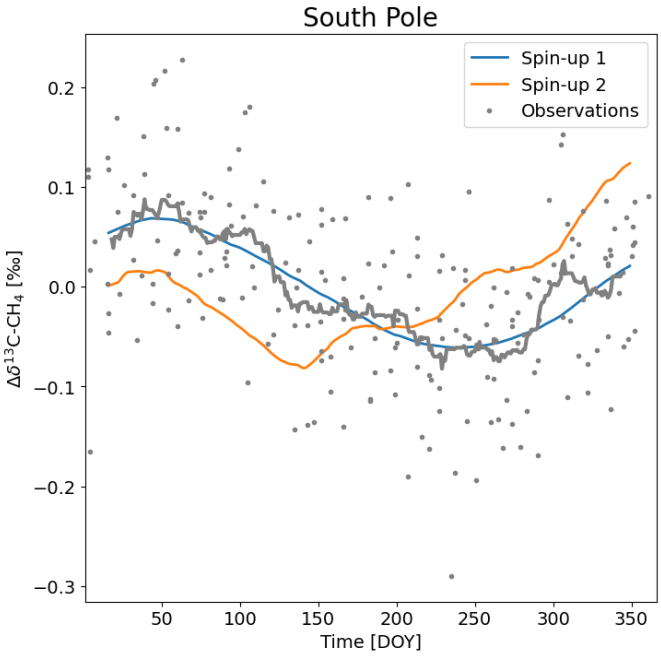

Figure S3. Modelled and observed average seasonal cycle at South Pole. Gray dots are individual observations between 2000–2006, and solid gray lines are 30-day moving averages of the observations. The colored lines are 30-day moving averages of the model estimates from spin-up simulations for year 2000 using original isotope signature values (Spin-up 1) and rounded signature values (Spin-up 2).

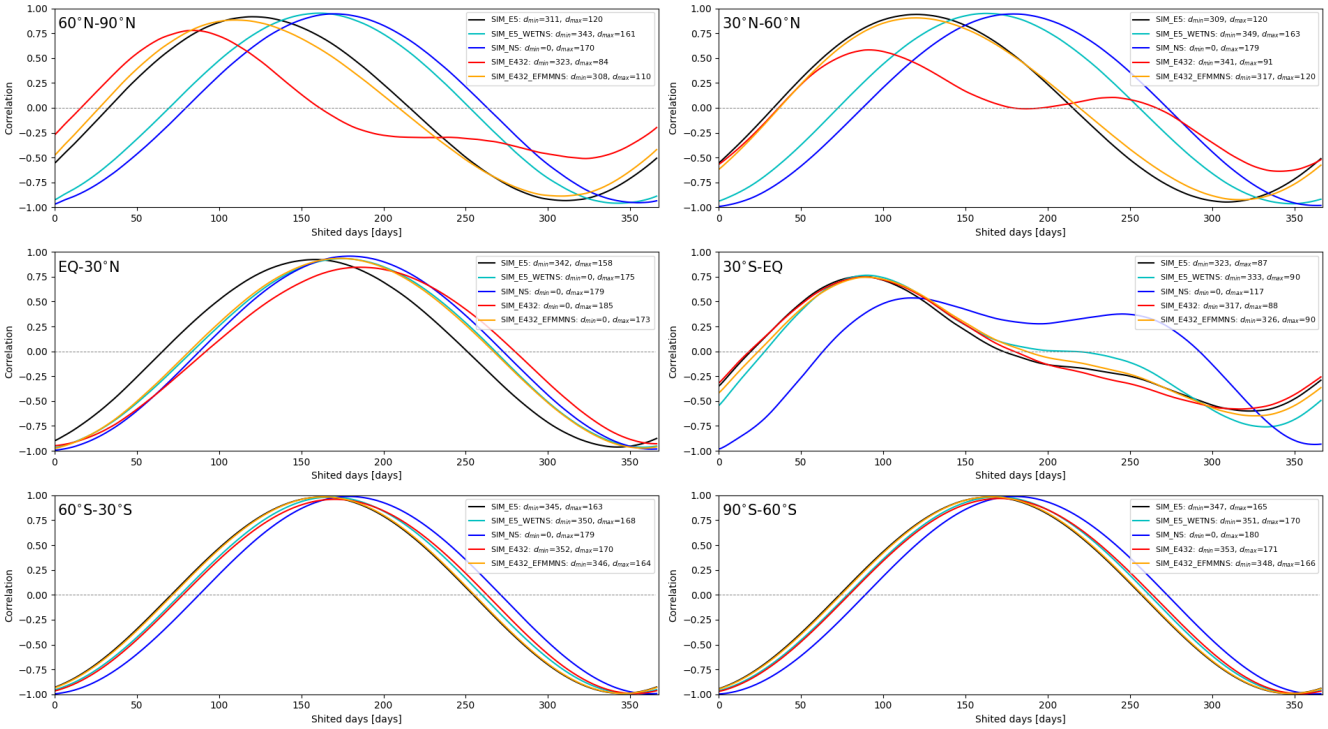

Figure S4. Shifted correlations of ΔCH_4 and $\Delta\delta^{13}C$, calculated from 2002-2012.

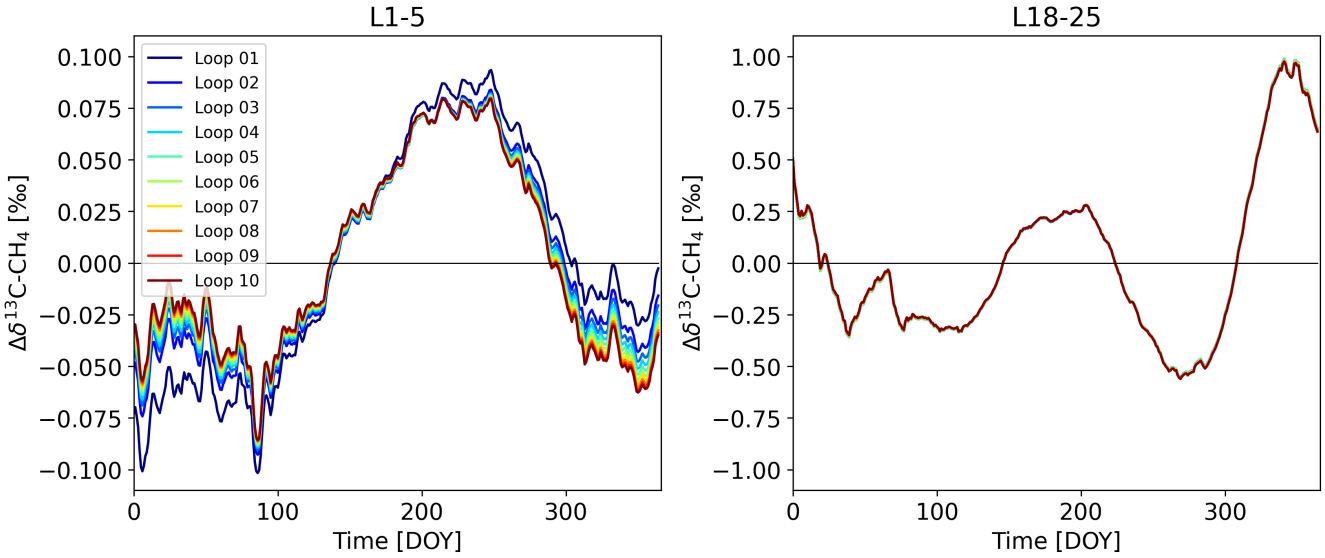

Figure S5. Detrended daily zonal mean $\Delta\delta^{13}\mathrm{C}$ at EQ–30° N, averaged over the lower most five layers (L1–5, troposphere) (top), and the upper most eight layers (L18–25, stratosphere) (bottom). The initial fields are taken from the 40-year spin-up using SIM_E5 setup, and the year 2000 are "looped" over 10 times using EDGAR v4.3.2 emission fields. This illustrates how long the seasonality takes to stabilise when using different emission fields to those used in the spin-up. Note the differences in y-axis.

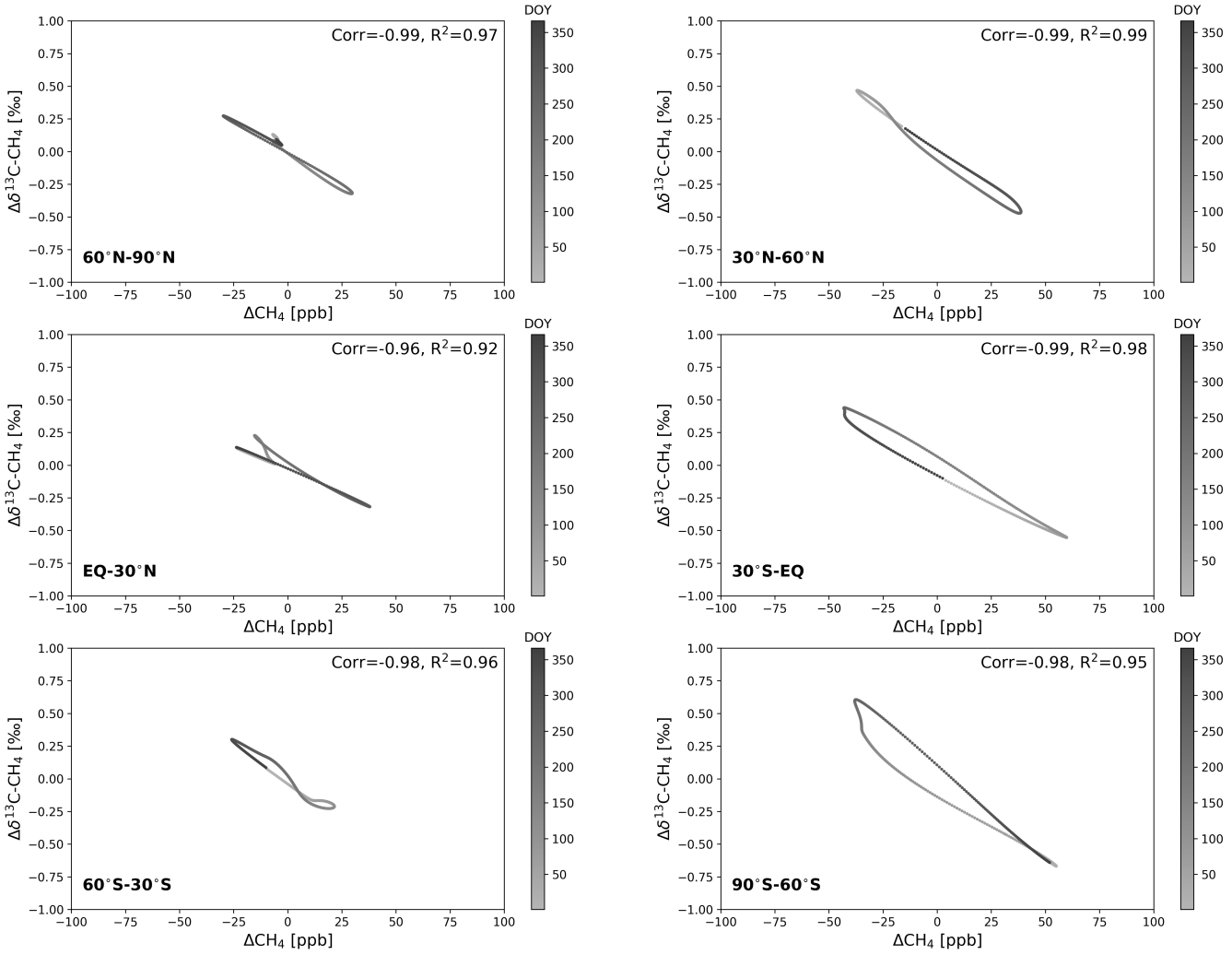

Figure S6. Detrended daily average $\Delta\mathrm{CH}_4$ against $\Delta\delta^{13}\mathrm{C}$ from the upper most 8 levels over 2002–2012 at 30° latitudinal bands. Color schemes indicate different simulations and the color darkness illustrates day of year (DOY). The lightest colors are DOY = 1 and the darkest DOY = 366.

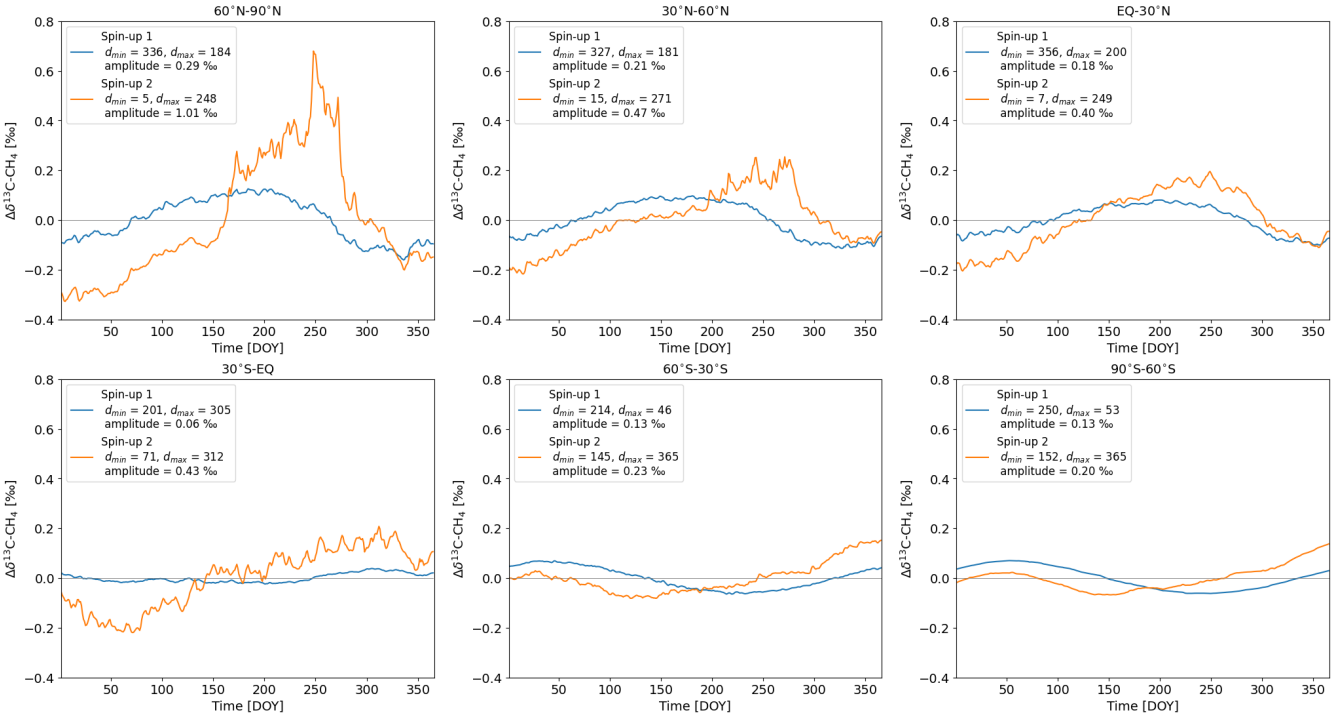

Figure S7. Detrended zonal mean $\Delta\delta^{13}$ from spin-up simulations for year 2000 using original isotope signature values (Spin-up 1) and rounded signature values (Spin-up 2). The timing of seasonal minimum and maximum days in DOY are shown as d_{min} and d_{max}, respectively.

References

Houghton, J. T., Meira Filho, L. G., Lim, K., Trennton, I., Mamaty, I., Bonduki, Y., Griggs, D. J., and Callander, B. A.: Revised 1996 IPCC Guidelines for National Greenhouse Gas Inventories, 1 - 3, 1997.